Turkish Journal of Electrical Engineering & Computer Sciences

http://journals.tubitak.gov.tr/elektrik/

Research Article

Turk J Elec Eng & Comp Sci
(2018) 26: 1599 – 1611

doi:10.3906/elk-1611-168

A novel DTC-SVM approach for two parallel-connected induction motors fed by matrix converter

Mahdi JAFARI[1], **Karim ABBASZADEH**[2,*], **Mustafa MOHAMMADIAN**[3]

[1]Department of Electrical Engineering, Faculty of Electrical Engineering, Science and Research Branch, Islamic Azad University, Tehran, Iran

[2]Department of Electrical Engineering, Faculty of Electrical Engineering, Khajeh Nassir-Al-Deen Toosi University of Technology, Tehran, Iran

[3]Department of Electrical Engineering, Faculty of Electrical Engineering, Tarbiat Modares University, Tehran, Iran

Received: 16.11.2016 • **Accepted/Published Online:** 28.06.2017 • **Final Version:** 30.05.2018

Abstract: AC machines fed by a single inverter are widely used in industries such as railroad electrification systems where speed synchronization does not have to be exact. The low cost and volume and the small number of power electronic components are attractive aspects of single-inverter multi-motor systems. This paper proposes a novel approach to controlling the speed and torque of two induction motors connected in parallel and fed by a matrix converter under unbalanced load condition. This single-inverter dual-motor (SIDM) drive uses average and differential values of speed and torque together with stator and rotor flux parameters based on the flux dead-beat scheme. An advantage of the proposed approach, compared with the conventional direct torque control (DTC) method, is that it eliminates the lookup table and lowers the torque and current ripple through the use of the PI controller instead of hysteresis blocks. Combining DTC and space vector modulation (SVM) with a matrix converter (MC) and achieving the unit input power factor are other advantages of the present study. The main purpose of this study was to propose a new drive system with an MC for two parallel-connected induction motors using the DTC method and SVM consisting of a flux dead-beat scheme.

Key words: Matrix converter, single-inverter dual-motor drive, DTC-SVM, dead-beat scheme

1. Introduction

Using a single inverter to control multiple motors has attracted much attention. This approach has such advantages as the small number of insulated-gate bipolar transistors (IGBTs) and the low weight and volume of the inverter, which decrease system complexity. This approach is preferred in cases where exact speed synchronization between motors is not required [1]. In many industrial applications, such as paper or steel rolling mills and railroad electrification systems, multiple motors are controlled simultaneously [2]. The motors can be connected in series or in parallel and can be controlled independently. It should be noted that the stator winding of two- or multiphase motors can be connected in series or in parallel, but in three-phase motors just parallel connection is possible [3].

The potential problems in the single-inverter dual-motor (SIDM) control are as follows: (1) when a common voltage vector is applied, stator flux in both motors is instantaneously placed in one direction, and (2) when unbalanced load condition occurs, the speed of the motors does not reach the desired point [4,5].

*Correspondence: abbaszadeh@kntu.ac.ir

Recently, there has been interest in dual-motor drives fed by a multiple-leg inverter. For example, the vector control method presented in [6] uses a four-leg inverter, and the approach introduced in [7,8] draws upon a five-leg inverter. Both types of inverters can feed the two motors with different voltage vectors. However, increasing the number of motors leads to an increase in the number of capacitors and IGBTs [9]. Another choice is the matrix converter (MC), which, like multilevel converters, provides a large number of voltage vectors for modulation. The main advantages of the MC are the ability to generate sinusoidal input–output voltage and current and the possibility of adjusting input power factor [10,11]. The MC is recommended for extreme temperature conditions and critical volume/weight applications [12].

Two key considerations in SIDM systems are control and modulation. The existing control strategies are essentially of two main types:

1) The master–slave (MS) pattern, which is preferred in identical machines. In this pattern, in order to maintain the stator flux at its nominal value, the motor with the greatest stator flux magnitude is selected as the master, and the behavior of slave motors is not checked. However, the problem with this choice is that the behavior of slave motors may not be acceptable in some conditions [1,4].

2) The mean control pattern, where the average and differential values of the speed and current of the motors are calculated. A significant drawback of this choice is that the stator flux of any of the motors may exceed the reference value [4].

Furthermore, there is a third pattern, which is a combination of the above-mentioned patterns [1].

Each of the patterns discussed above can be implemented via vector control or direct torque control (DTC) methods. Most of the studies into SIDM systems have focused on the former. For instance, Matsuse in [13] proposed a sensorless vector control method on the basis of the mean value pattern and the sum of the torque values of two induction motors using a three-leg inverter. Furthermore, [14] compared the effect of the P controller with that of the PI controller in the torque control loop. Moreover, the weighted vector control method propounded in [2] can improve the speed characteristics and start-up conditions of both motors. Study [15] replicated [2] taking account of differences in torque values and obtained better results. The authors of [16] proposed a straightforward method on the basis of direct vector control for two parallel-connected induction motors fed by a single inverter.

The use of the DTC method in SIDM has been the subject of a few studies. Study [17] proposed a method according to the MS pattern and based on the conventional DTC method to control a system consisting of two permanent magnet synchronous motors fed by a three-leg inverter. The DTC approach provides easier torque control, allows fast dynamic response, and does not require rotary coordinate transformation and independence of motor parameters [18]. However, it has more torque and current ripple [19]. One of the solutions to this problem is space vector modulation (SVM), which provides continuous space vector for voltage modulation [20].

A review of the existing literature reveals that using the MS pattern implemented via the DTC method yields better results than the situation where it is implemented via the vector control method. However, the opposite is true for the mean control pattern [1].

There is no report, to the best of our knowledge, of the use of DTC-SVM in SIDM systems fed by an MC. The present study was an attempt to combine the mean control pattern and the DTC approach with SVM via the flux dead-beat scheme so as to find reference voltage vector equations for two induction motors fed by an MC. This combination enables the SIDM drive to reduce torque and current ripple and to obtain the unit input

power factor. Therefore, it improves the control performance of the drive system. In addition, if resistance voltage drop is ignored, the calculations required to generate the proper control voltage vector are simplified. Moreover, the propounded approach eliminates the lookup table and the nonlinearity effect of the hysteresis blocks through the use of the PI controller.

The purpose of the study reported here is threefold: (1) to introduce a novel drive system with a matrix converter for two parallel-connected induction motors through the DTC-SVM method with a flux dead-beat scheme; (2) to lower the torque ripple more than does the conventional DTC; and (3) to maintain the stability of motor speed under unbalanced load circumstances. The remainder of the paper is as follows. In Section 2, the proposed control method is delineated. Section 3 presents and discusses the simulation results. Finally, conclusions are given in Section 4.

2. The proposed DTC-SVM method

A solution put forward to control SIDM drives on the basis of the conventional DTC fed by an MC makes it possible to generate the voltage vectors necessary for the implementation of the DTC of two motors under the constraint unity input power factor. In this method, two different tables are established depending on the position of the stator flux vectors of the motors in relation to each other and, in other words, according to whether the two vectors are located in the same sector or in two adjacent sectors. Eventually, based on the output of the hysteresis blocks of the torque and flux, two lookup tables are drawn [17]. If two-level hysteresis blocks are used, there will be 16 states in the lookup tables, and 36 states if three-level blocks are used. Due to the changes in the hysteresis bands of the torque and flux and variations in motor speed, the switching frequency will be variable, and this will increase torque ripple. The present study seeks to propose a new DTC-SVM method that, while enjoying the benefits of the conventional DTC method, is capable of coping with the problem involved. Although the proposed method is more difficult to implement, it can significantly reduce the torque ripple.

2.1. Induction motor equations

An induction motor in the synchronous reference frame can be described using the following flux and voltage equations [20]:

$$\lambda_s^e = L_s \mathbf{i}_s^e + L_m \mathbf{i}_r^e \tag{1}$$

$$\lambda_r^e = L_m \mathbf{i}_\mathbf{s}^\mathbf{e} + L_r \mathbf{i}_\mathbf{r}^\mathbf{e} \tag{2}$$

$$\mathbf{V}_\mathbf{s}^\mathbf{e} = R_s \mathbf{i}_\mathbf{s}^\mathbf{e} + \frac{d}{dt}\lambda_\mathbf{s}^\mathbf{e} + j\omega_e \lambda_\mathbf{s}^\mathbf{e} \tag{3}$$

$$0 = R_r \mathbf{i}_\mathbf{r}^\mathbf{e} + \frac{d}{dt}\lambda_\mathbf{r}^\mathbf{e} + j(\omega_e - \omega_r)\lambda_\mathbf{r}^\mathbf{e}, \tag{4}$$

where λ_s^e is the stator flux vector, λ_r^e represents the rotor flux vector, $\mathbf{i}_s^e$ indicates the stator current vector, $\mathbf{i}_r^e$ is the rotor current vector, $\mathbf{V}_\mathbf{s}^\mathbf{e}$ denotes the stator voltage vector, ω_e and ω_r are the angular frequency of the inverter and rotor, respectively, L_s and L_r are the self-inductance of the stator rotor, in that order, and finally L_m represents mutual inductance.

Considering the parameter $\beta = \frac{L_m}{L_r}$, the above equations can be rewritten as follows [20]:

$$\lambda_{\mathbf{s}}^{\mathbf{e}} = L_s \mathbf{i}_{\mathbf{s}}^{\mathbf{e}} + L_m^{'} \mathbf{i}_{\mathbf{r}}^{\mathbf{e}'} , \quad \lambda_{\mathbf{r}}^{\mathbf{e}'} = \mathbf{L}_{\mathbf{m}}^{'} \mathbf{i}_{\mathbf{s}}^{\mathbf{e}} + \mathbf{L}_{\mathbf{r}}^{'} \mathbf{i}_{\mathbf{r}}^{\mathbf{e}'} \tag{5}$$

$$\mathbf{V}_{\mathbf{s}}^{\mathbf{e}} = R_s \mathbf{i}_{\mathbf{s}}^{\mathbf{e}} + \frac{d}{dt} \lambda_{\mathbf{s}}^{\mathbf{e}} + j\omega_e \lambda_{\mathbf{s}}^{\mathbf{e}} \ , \ 0 = R_r^{'} \mathbf{i}_{\mathbf{r}}^{\mathbf{e}'} + \frac{d}{dt} \lambda_{\mathbf{r}}^{\mathbf{e}'} + j(\omega_e - \omega_r) \lambda_{\mathbf{r}}^{\mathbf{e}'} \tag{6}$$

where $\lambda_{\mathbf{r}}^{\mathbf{e}'} = \beta \lambda_r^e$, $\mathbf{i}_{\mathbf{r}}^{\mathbf{e}'} = (1/\beta) \mathbf{i}_{\mathbf{r}}^{\mathbf{e}}$, and $L_m^{'} = \beta^2 L_r$, $R_r^{'} = \beta^2 R_r$

The leakage flux vector is defined in (7):

$$\lambda_{\sigma}^{\mathbf{e}} = L_{\sigma} \mathbf{i}_{\mathbf{s}}^{\mathbf{e}} = \lambda_{\mathbf{s}}^{\mathbf{e}} - \lambda_{\mathbf{r}}^{\mathbf{e}'} \tag{7}$$

where $L_{\sigma} = \sigma L_s = L_s - L_r^{'}$

State equations can be rearranged in the following form using the equations above [20]:

$$\frac{d}{dt} \begin{bmatrix} \lambda_{\mathbf{s}}^{\mathbf{e}} \\ \lambda_{\mathbf{r}}^{\mathbf{e}'} \end{bmatrix} = \begin{bmatrix} -(1/\tau_s)\mathbf{I} - \omega_e \mathbf{J} & \left(1/\tau_s^{'}\right)\mathbf{I} \\ \left(\frac{1-\sigma}{\tau_r}\right)\mathbf{I} & -\left(1/\tau_r^{'}\right)\mathbf{I} - (\omega_e - \omega_r)\mathbf{J} \end{bmatrix} \begin{bmatrix} \lambda_{\mathbf{s}}^{\mathbf{e}} \\ \lambda_{\mathbf{r}}^{\mathbf{e}'} \end{bmatrix} + \begin{bmatrix} I \\ 0 \end{bmatrix} \mathbf{V}_{\mathbf{s}}^{\mathbf{e}} = \mathbf{A}^e \mathbf{X}^{\mathbf{e}} + \mathbf{B} \mathbf{V}_{\mathbf{s}}^{\mathbf{e}} \tag{8}$$

$$\lambda_{\sigma}^{\mathbf{e}} = \begin{bmatrix} \mathbf{I} & -\mathbf{I} \end{bmatrix} \mathbf{X}^{\mathbf{e}} = C \mathbf{X}^{\mathbf{e}} \tag{9}$$

where

$\tau_s^{'} = \frac{L_{\sigma}}{R_s} = \frac{\sigma L_s}{R_s}$, $\tau_r^{'} = \sigma \tau_r$, $\mathbf{I} = \begin{bmatrix} 1 & 0 \\ 0 & 1 \end{bmatrix}$, $\mathbf{J} = \begin{bmatrix} 0 & -1 \\ 1 & 0 \end{bmatrix}$

By introducing $\tilde{X}^e$ as (10), the stator equation can be written as (11):

$$\tilde{X}^e = \begin{bmatrix} \lambda_{\mathbf{s}}^{\mathbf{e}} \\ \lambda_{\sigma}^{\mathbf{e}} \end{bmatrix} = \begin{bmatrix} I & 0 \\ I & -I \end{bmatrix} \tag{10}$$

$$\frac{d}{dt} \tilde{X}^e = \frac{d}{dt} \begin{bmatrix} \lambda_{\mathbf{s}}^{\mathbf{e}} \\ \lambda_{\sigma}^{\mathbf{e}} \end{bmatrix} = \begin{bmatrix} -\omega_e J & -\left(1/\tau_s^{'}\right) I \\ \left(\frac{1}{\tau_r}\right) I - \omega_r J & -\left(1/\tau_r^{'} + 1/\tau_s^{'}\right) I - (\omega_e - \omega_r) J \end{bmatrix} \begin{bmatrix} \lambda_{\mathbf{s}}^{\mathbf{e}} \\ \lambda_{\mathbf{r}}^{\mathbf{e}'} \end{bmatrix} + \begin{bmatrix} I \\ 0 \end{bmatrix} \mathbf{V}_{\mathbf{s}}^{\mathbf{e}} \tag{11}$$

Eq. (11) can be approximated as (12) by eliminating voltage drops caused by the stator and rotor resistance [20].

$$\frac{d}{dt} \tilde{X}_{dq} = \frac{d}{dt} \begin{bmatrix} \lambda_{\mathbf{s}}^{\mathbf{e}} \\ \lambda_{\sigma}^{\mathbf{e}} \end{bmatrix} = \begin{bmatrix} -\omega_e J & 0 \\ -\omega_r J & -(\omega_s - \omega_r) J \end{bmatrix} \tilde{X}_{dq} + \begin{bmatrix} I \\ I \end{bmatrix} \mathbf{V}_{\mathbf{dq}}^{\mathbf{e}} \tag{12}$$

Parameters in (12) are defined as follows:

$$\frac{d}{dt} |\lambda_s| = \mathbf{V}_d,$$

$$0 = -\omega_e |\lambda_s| + \mathbf{V}_q ,$$

$$\frac{d}{dt}\lambda_{\sigma d} = (\omega_e - \omega_r)\,\lambda_{\sigma q} + \mathbf{V}_d$$

$$\frac{d}{dt}\lambda_{\sigma q} = -\omega_r\,|\lambda_s| - (\omega_e - \omega_r)\,\lambda_{\sigma d} + \mathbf{V}_q \tag{13}$$

The electromagnetic torque can be determined by multiplying stator and rotor flux components together as (14) [20]:

$$\mathbf{T}_e = \frac{3}{2}P\lambda_s \times \mathbf{i}_s = \frac{3}{2}P\frac{L_m}{\sigma L_s L_r}\lambda_r \times \lambda_s = \frac{3}{2}P\frac{L_m}{\sigma L_s L_r}\,|\lambda_s|\,|\lambda_r|\,sin\theta$$

$$\mathbf{T}_e = \frac{3}{2}P\,|\lambda_s|\left|\lambda_r^{'}\right| \times \frac{sin\delta}{L_\delta} = \frac{3}{2}P\,|\lambda_s|\,\lambda_{\sigma q}/L_\sigma \tag{14}$$

λ_r in relation to the stator flux can be written as

$$\lambda_r = \frac{L_m}{L_r}\frac{1}{1+s\sigma\tau_r}\lambda_s \tag{15}$$

2.2. The proposed DTC-SVM using a flux dead-beat scheme

The flux dead-beat scheme helped minimize torque ripple in one sampling period T_sp by choosing the appropriate voltage vector.

Stator flux error is related to the applied voltage vector, as seen in (16) [20]:

$$\mathbf{V_S} = \frac{d\lambda_S}{dt} + R_S\mathbf{I}_S,\ \ \mathbf{V_k} = \frac{d\lambda_k}{T_s} = \left(\frac{\lambda_k^* - \lambda_{k-1}}{T_s}\right) + R_s\mathbf{I}_{k-1} \tag{16}$$

If (13) and (14) are applied to each motor, two equations are obtained. These equations are combined so that the average references $\bar{V_d^{e*}}$ and $\bar{V_q^{e*}}$ are calculated as follows:

$$\bar{V_d^{e*}} = \frac{\left(\left|\bar{\lambda_s^*}\right| - \left|\bar{\lambda_s}\right|\right)}{Ts} \tag{17}$$

$$\bar{V_q^{e*}} = \frac{1}{T_s}\left[\left(\frac{\left|\bar{\lambda_s^*}\right|}{\bar{\lambda_{rd}^{'}}}\right)\left(\bar{\lambda_{\sigma q}^*} - \bar{\lambda_{\sigma q}}\right) + \frac{\left(\left|\bar{\lambda_s^*}\right| \times \left(\bar{\lambda_{\sigma q}} - \bar{\lambda_{\sigma q}^*}\right)\right)}{\bar{\lambda_{rd}^{'}}} - \frac{\left(|\lambda_{s2}^*| \times \left(\lambda_{\sigma q2}^* - \lambda_{\sigma q2}\right)\right)}{2\lambda_{rd2}^{'}} - \frac{\left(|\lambda_{s1}^*| \times \left(\lambda_{\sigma q1}^* - \lambda_{\sigma q1}\right)\right)}{2\lambda_{rd1}^{'}}\right]$$
$$+ \bar{\omega_r}\left|\bar{\lambda_s}\right| + \Delta\omega_r\Delta\,|\lambda_s| \tag{18}$$

$$\bar{\lambda_{\sigma q}^*} = \frac{3}{2}P\left[\frac{L\sigma_1 T_{e1}}{2\,|\lambda_{s1}^*|} + \frac{L\sigma_2 T_{e2}}{2\,|\lambda_{s2}^*|} - \frac{\bar{L_\sigma}\bar{T_e}}{2\left|\bar{\lambda_s^*}\right|}\right], \tag{19}$$

where

$$\left|\bar{\lambda_s}\right| = \frac{|\lambda_{s1}^e| + |\lambda_{s2}^e|}{2},\ \bar{\lambda_{\sigma q}} = \frac{\lambda_{\sigma q1}^e + \lambda_{\sigma q2}^e}{2},\ \bar{\lambda_{rd}^{'}} = \frac{\lambda_{\sigma q1}^e + \lambda_{\sigma q2}^e}{2},\ \bar{\omega_r} = \frac{\omega_{r1} + \omega_{r2}}{2} \tag{20}$$

$$\bar{T_e} = \frac{T_{e1} + T_{e2}}{2},\ \ \bar{L_\sigma} = \frac{L_{\sigma 1} + L_{\sigma 2}}{2},\ \Delta\omega_r = \frac{\omega_1 + \omega_2}{2},\ \Delta\,|\lambda_s| = \frac{|\lambda_{s1}^e| - |\lambda_{s2}^e|}{2} \tag{21}$$

The flux linkage space vectors of the two induction motors are illustrated in Figure 1.

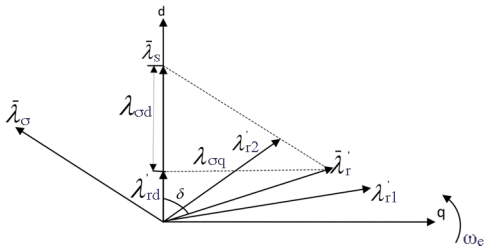

Figure 1. Flux-linkage space vector of dual induction motors.

2.3. System configuration in the proposed DTC-SVM

The proposed method entails four main steps (Figure 2). First, the values of stator and rotor flux are calculated via Eq. (15). Then $\lambda^{*}_{\sigma q}$ is calculated by putting the reference torque value, which is the output of the PI controller, in (19). Subsequently, the voltage vector is calculated in the synchronous reference frame using (17) and (18). Finally, the angle of input voltage vector is calculated in order to obtain unit input power factor. The magnitude and phase angle of the reference voltage vector are sent to the SVM modulator to issue proper commands to the MC [21].

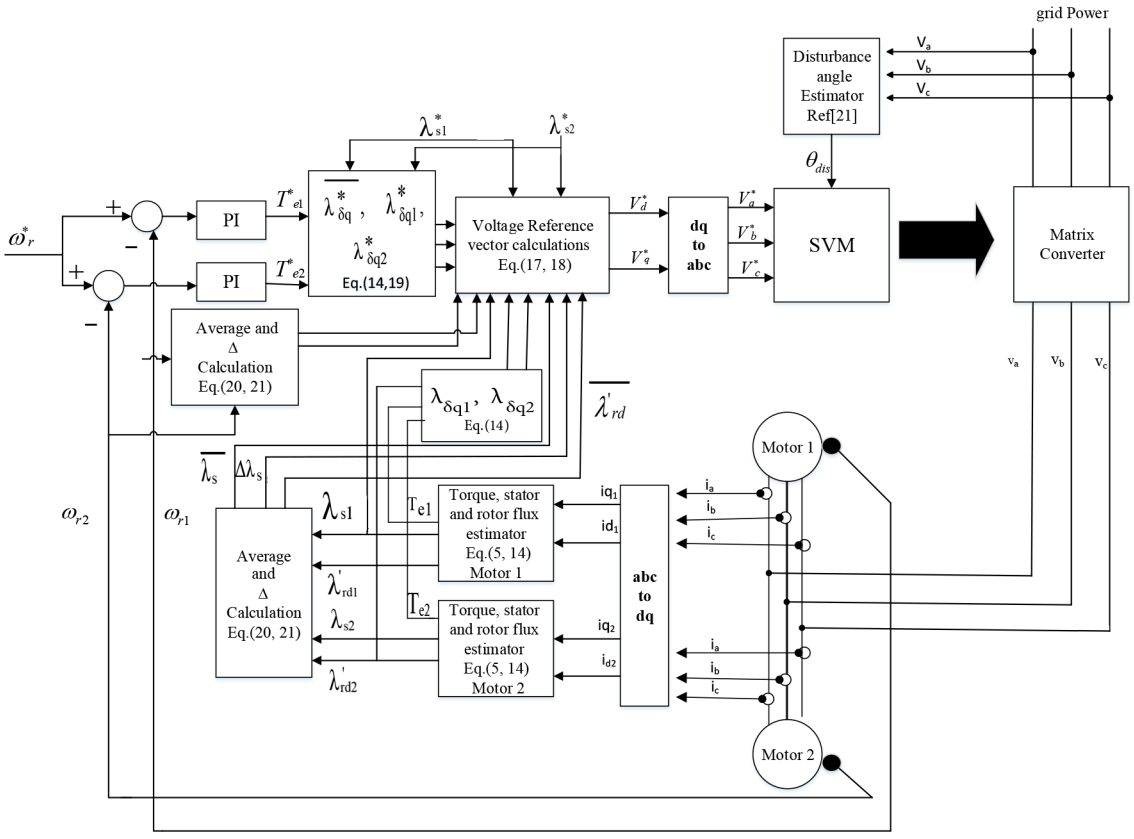

Figure 2. Proposed DTC-SVM for dual induction motors fed by MC.

3. Results and discussion

The proposed DTC-SVM method was compared with the conventional DTC method via some numerical simulations in order to study the steady-state and dynamic performance. The reference value for stator flux is the motor nominal flux. The machines under investigation were two 200-hp, 4-pole, 460-V $_L$, and 60-Hz squirrel cage induction motors with $R_s = 0.0148\ \Omega$, $R_r = 0.0092\ \Omega$, $L_{ls} = 0.003$ H, $L_{lr} = 0.003$ H, and $L_m = 0.01$ H.

3.1. Unbalanced load test

The conventional and proposed methods were subjected to the unbalanced load condition. The speeds of the motors were set at 1000 rpm, and both motors were started under no-load condition. After 1.2 s, torque values of 400 Nm and 200 Nm were applied to Motor 1 and Motor 2, respectively. The simulation results are presented in Figures 3 and 4, in that order. Figures 5 and 6 show more details about the speed curves. As can be seen, in both methods, both motors followed the torque command. Furthermore, fluctuations can be observed in the torque curve for 0.2 s after the occurrence of step change in the load. In the propounded method, these fluctuations occurred in the motor subjected to the lower load, while in the conventional approach the

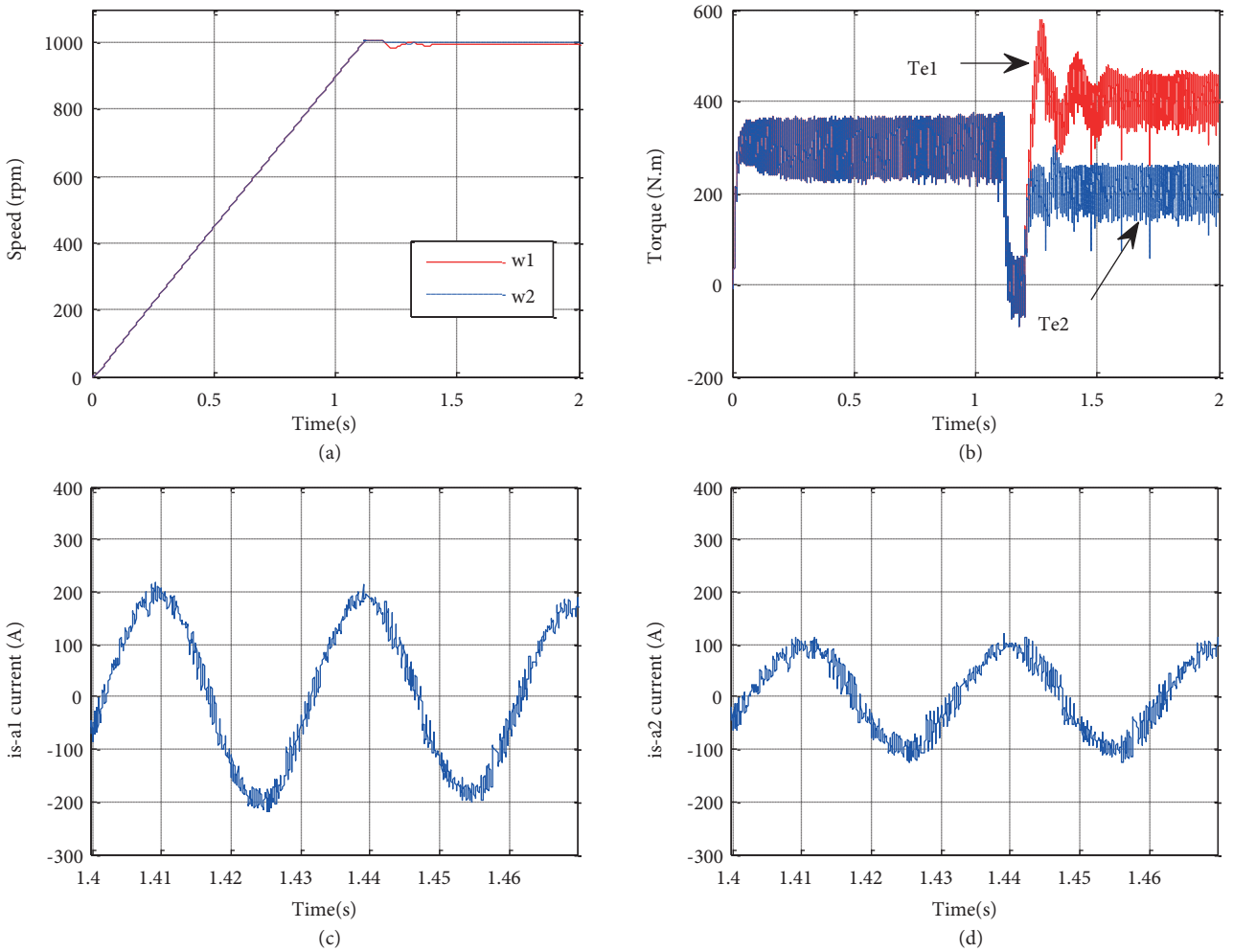

Figure 3. Simulation results under unbalanced load condition in conventional DTC: a) Speed of motors; b) Torque of motor; c) Current of Motor 1; d) Current of Motor 2.

fluctuations took place in the motor under higher load. Lastly, in our method, the curves of the two motors reached the final point faster. According to Figures 3b and 4b, torque ripple was reduced significantly in the proposed approach.

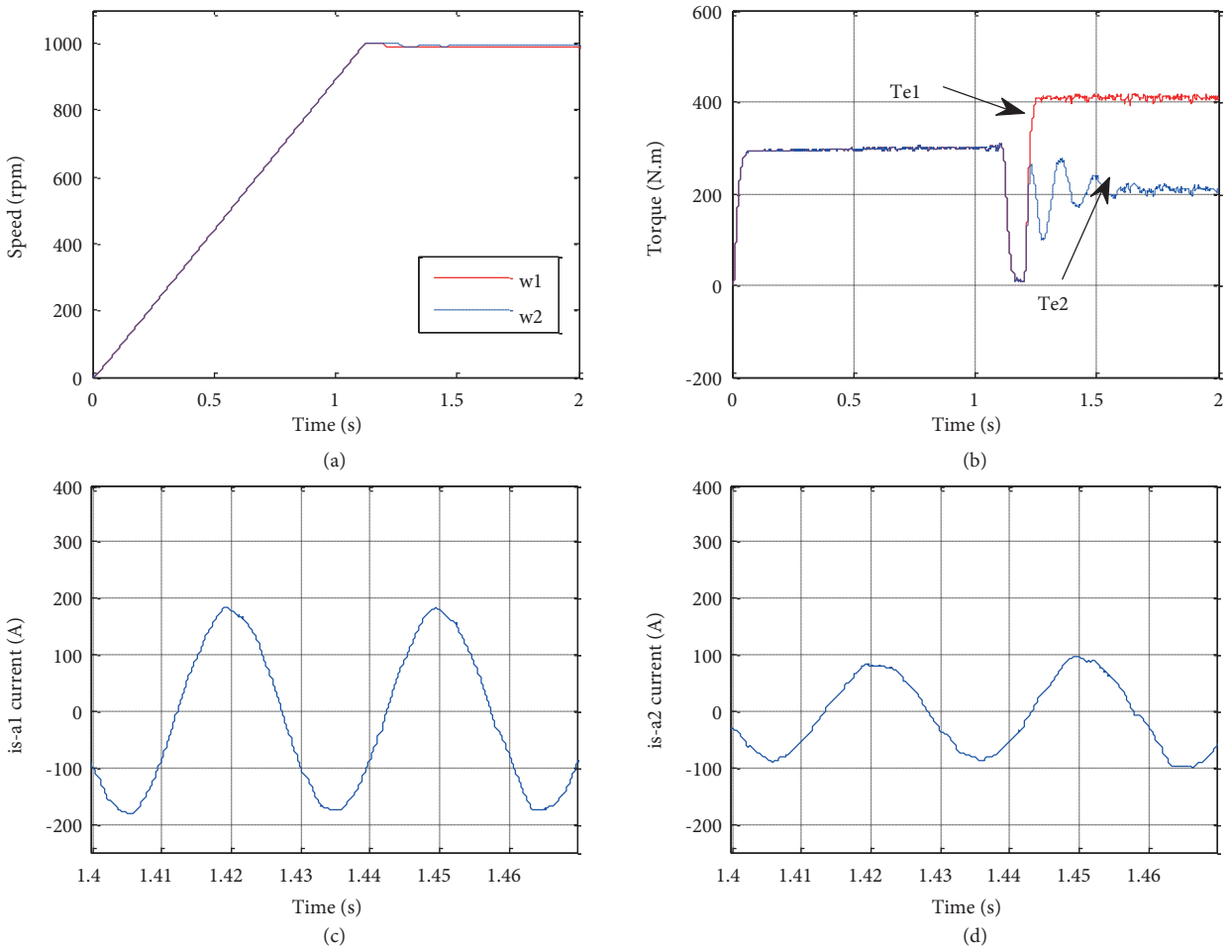

Figure 4. Simulation results under unbalanced load condition in the proposed DTC: a) speed of motors; b) Torque of motors; c) Current of Motor 1; d) Current of Motor 2.

3.2. Change in speed step under unbalanced load condition

An investigation was made into the effect of changes in the reference speed on the transient and steady-state performance in the proposed DTC method. Both motors were started under no-load condition, but the load of Motor 1 was changed to 400 Nm after 2 s. After 4 s, when the reference speed was changed from 500 rpm to 1000, both motors followed the speed command closely.

According to Eq. (22), at t = 4 s, due to the increase in the speed of motors, $\frac{d\omega}{dt} > 0$, and consequently the torque of motors would be more than the reference torque value.

$$T_e - T_l = J\frac{d\omega}{dt}, \tag{22}$$

where J is motor inertia.

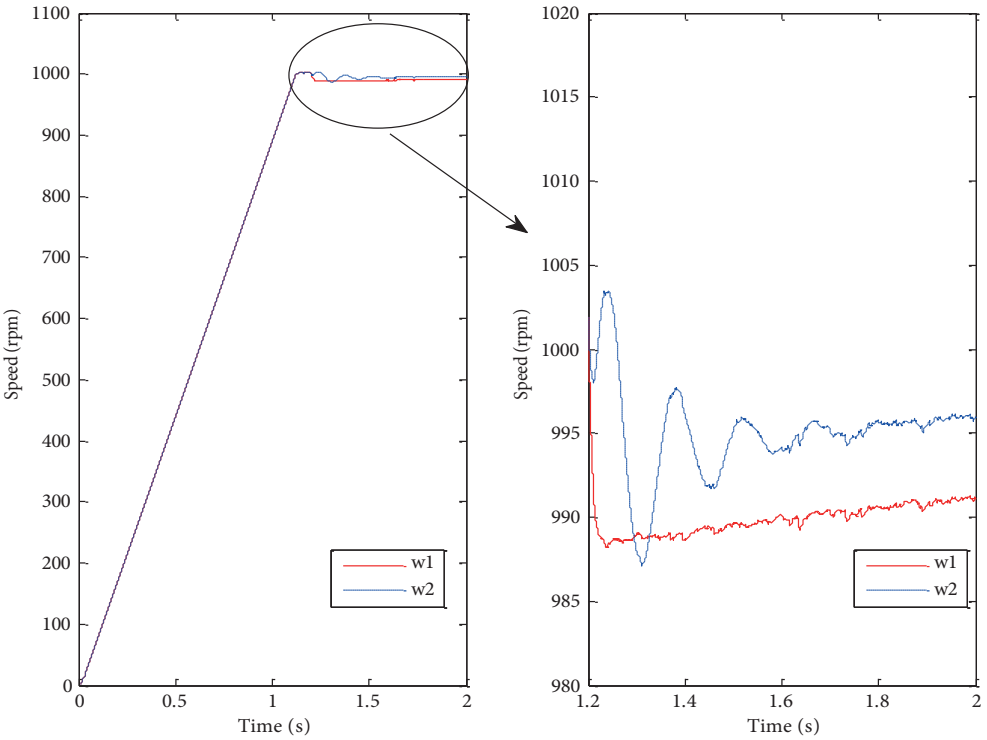

Figure 5. Speed of motors under unbalanced load condition in conventional DTC.

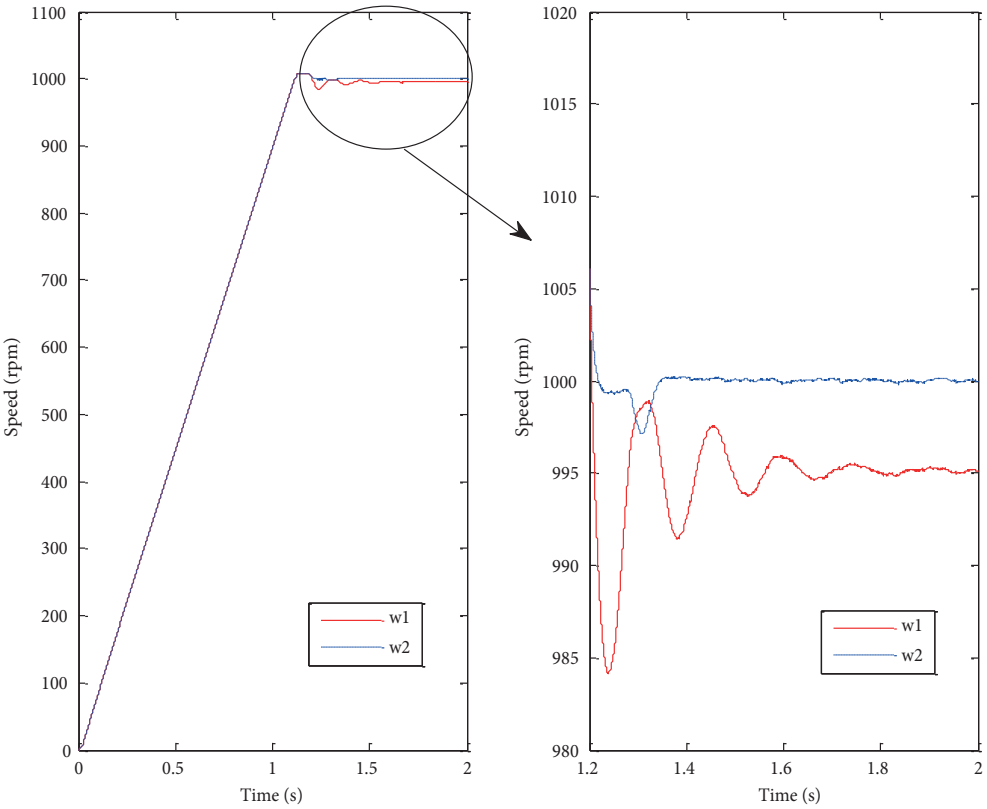

Figure 6. Speed of motors under unbalanced load condition in the proposed DTC.

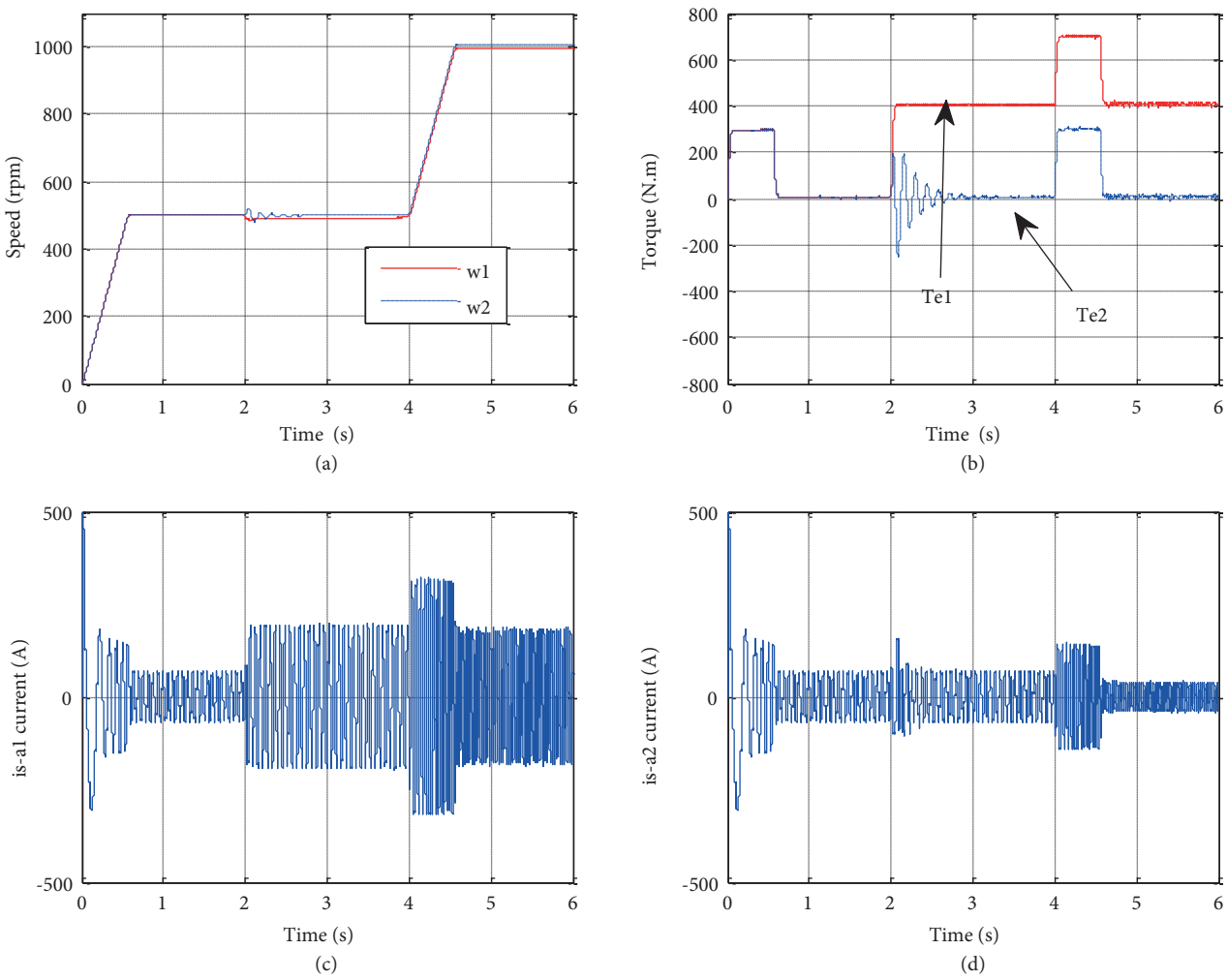

Figure 7. Speed step command under unbalanced load condition in the proposed DTC: a) motor speed; b) motor torque; c) stator current of Motor 1; d) stator current of Motor 2.

Figure 7 illustrates the characteristics of both motors in this condition. Fluctuations can be seen in the torque curve of Motor 2 for 0.8 s, but fluctuations were damped in the steady-state condition.

3.3. Dynamic performance during a change in torque command

Figure 8 emphasizes the ability of the proposed method to generate electrical power when motors brake in low speed condition. This section can also be done with nominal speed, but it emphasizes the proposed system ability at low speed under regeneration condition. According to Figure 8, torque was changed from +400 Nm to –400 Nm after 3 s, with speed being set at 500 rpm. The torque of two motors demonstrates appropriate response and current waveform has regained sinusoidal form immediately after step change. Moreover, the speed followed the reference values very well.

As can be seen in Figure 9, sinusoidal voltage is in phase with the corresponding filtered current at the input side of the MC, and this confirms the validity of the propounded DTC-SVM approach to operate under unit input power factor. When the torque command changes, the direction of motor current changes. Therefore, the phase angle difference between input current and corresponding voltage is about π radians, indicating that

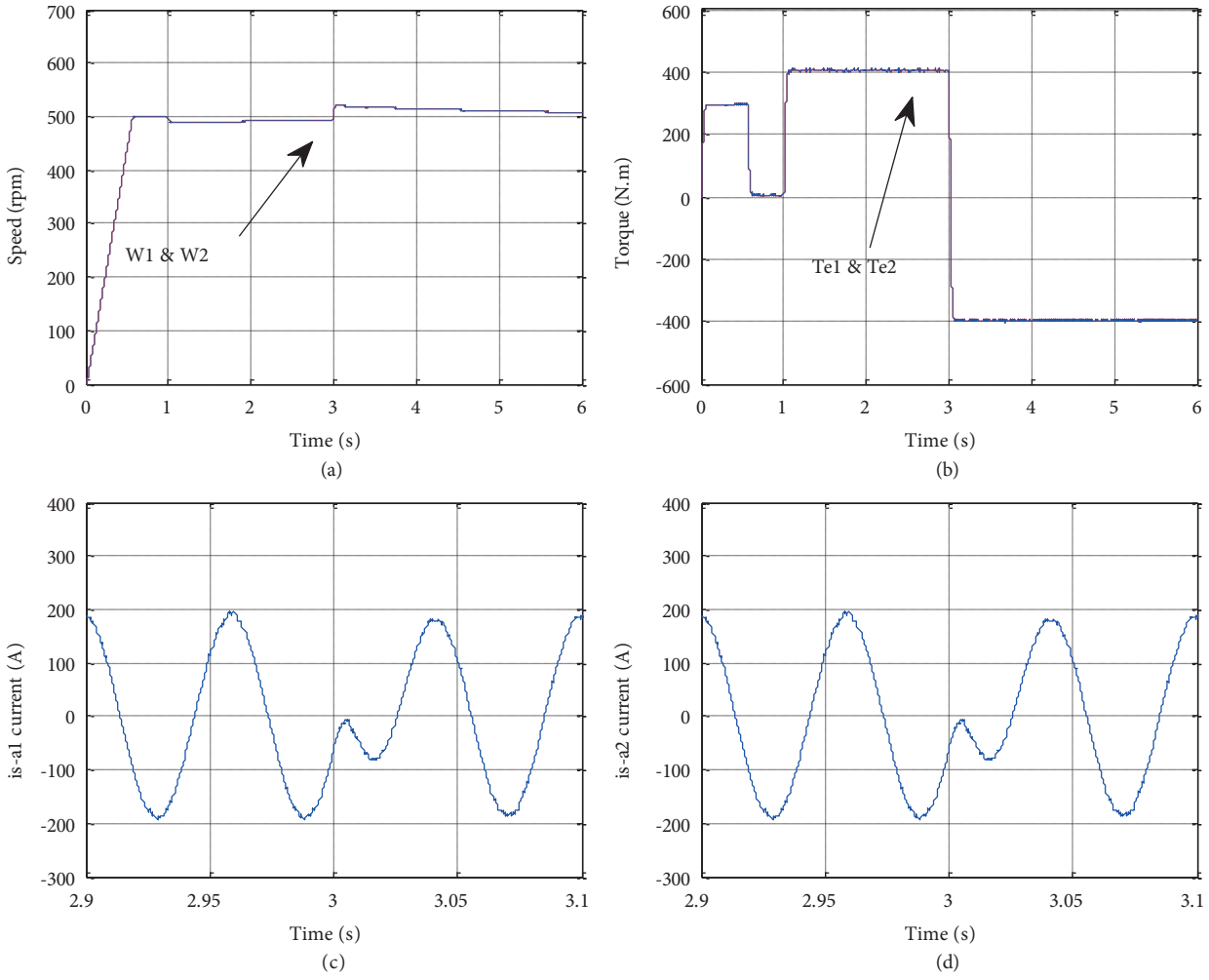

Figure 8. Torque step command from +400 Nm to –400 Nm at 500 rpm in the proposed DTC: a) motor speed; b) motor torque; c) stator current of Motor 1; d) stator current of Motor 2.

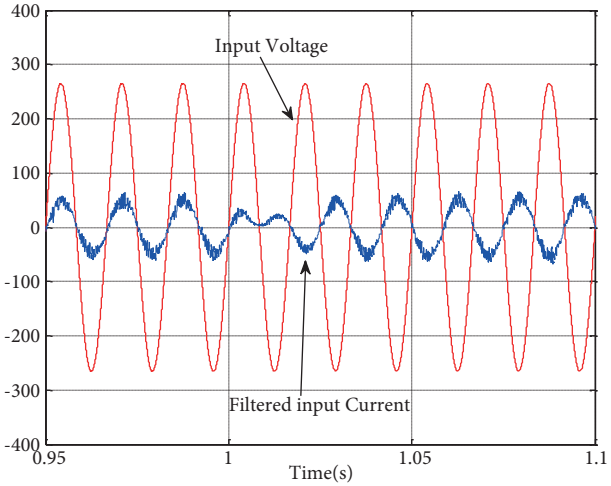

Figure 9. Input voltage and filtered input current waveform at 500 rpm during torque step command from +400 Nm to –400 Nm in the proposed DTC.

the machines now generate electrical power. It is worth noting that, in this case, motor speed is higher than the reference speed because slip is higher than 1.

4. Conclusions

This study drew upon average and differential values of speed and torque and also stator and rotor flux parameters based on the flux dead-beat scheme to control two parallel-connected induction motors fed by an MC under unbalanced load condition. This new DTC-SVM method eliminates the lookup table and reduces the torque and current ripple by replacing hysteresis blocks with the PI controller. Another advantage of the propounded approach is that it achieves the unit input power factor. Lastly, this method is capable of maintaining the stability of motor speed under unbalanced load conditions.

References

[1] Joshi BM, Chandorkar MC. Vector control of two-motor single-inverter induction machine drives. Electr Pow Compo Sys 2014; 42: 1158-1171.

[2] Xu F, Shi L, Li Y. The weighted vector control of speed-irrelevant dual induction motors fed by the single inverter. IEEE T Power Electr 2013; 12: 5665-5672.

[3] Jones M, Levi E, Iqbal A. Vector control of a five-phase series-connected two-motor drive using synchronous current controllers. Electr Pow Compo Sys 2005; 33: 411-430.

[4] Mohktari H, Alizadeh A. A new multi-machine control system based on Direct Torque Control algorithm. In: IEEE 2007 International Conference on Power Electronics; 22 October 2007; Daegu, Korea (South): IEEE. pp. 1103-1108.

[5] Joshi BM, Chandorkar MC. Effect of machine asymmetry on a two-machine direct torque controlled induction motor drive. In: EPE 2011 Proceedings of 14th European Conference on Power Electronics and Applications; 30 August–1 September 2011; Birmingham, UK: IEEE. pp. 1-10.

[6] Ninad NA, Lopes L. Per-phase vector control strategy for a four-leg voltage source inverter operating with highly unbalanced loads in stand-alone hybrid systems. Int J Elec Power 2014; 55: 449-459.

[7] Nguyen TD, Lee HH. Development of a three-to-five-phase indirect matrix converter with carrier-based PWM based on space-vector modulation analysis. IEEE T Ind Electron 2016; 63: 13-24.

[8] Lim CS, Rahim NA, Hew WP, Levi E. Model predictive control of a two-motor drive with five-leg-inverter supply. IEEE T Ind Electron 2013; 60: 54-65.

[9] Matsuse K, Kezuka N, Oka K. Characteristics of independent two induction motor drives fed by a four-leg inverter. IEEE T Ind Appl 2011; 47: 2125-2134.

[10] You K, Xiao D, Rahman MF, Uddin MN. Applying reduced general direct space vector modulation approach of AC–AC matrix converter theory to achieve direct power factor controlled three-phase AC–DC matrix rectifier. IEEE T Ind Appl 2014; 50: 2243-2257.

[11] Friedli T, Kolar JW. Milestones in matrix converter research. IEEJ J Ind Appl 2012; 1: 2-14.

[12] Friedli T, Kolar JW. Comprehensive comparison of three-phase AC-AC matrix converter and voltage DC-Link back-to-back converter systems. In: IEEE 2010 International Power Electronics Conference (IPEC); 21 June 2010; Sapporo, Japan: IEEE. pp. 2789-2798.

[13] Matsuse K, Kawai H, Kouno Y, Oikawa J. Characteristics of speed sensor less vector controlled dual induction motor drive connected in parallel fed by a single inverter. IEEE T Ind Appl 2004; 40: 153-1561.

[14] Matsuse K, Kouno Y, Kawai H, Yokomizo S. A speed-sensorless vector control method of parallel-connected dual induction motor fed by a single inverter. IEEE T Ind Appl 2002; 38: 1566-1571.

[15] Xu F, Shi L, Wang K, Li Y. A control strategy of dual induction motors fed by single inverter for traction system. In: IEEE Transportation Electrification Conference and Expo, Asia-Pacific (ITEC Asia-Pacific); 31 August 2014; Beijing, China: IEEE. pp. 1-6.

[16] Gunabalan R, Sanjeevikumar P, Blaabjerg F, Ojo O, Subbiah V. Analysis and implementation of parallel connected two-induction motor single-inverter drive by direct vector control for industrial application. IEEE T Power Electr 2015; 30: 6472-6475.

[17] Maurice F, Ngoc LN, Ana L. Direct torque control – a solution for mono inverter-dual parallel PMSM system. In: 21st Mediterranean Conference on Control and Automation; 25–28 June 2013; Platanias-Chania, Crete, Greece: IEEE. pp. 1477-1483.

[18] Xiao D, Rahman MF. A novel hysteresis direct torque control for matrix converter drives. EPE J 2011; 21: 40-48.

[19] Casadei D, Profumo F, Serra G, Tani A. FOC and DTC: two viable schemes for induction motors torque control. IEEE T Power Electr 2002; 17: 779-787.

[20] Lee KB, Blaabjerg F. Sensorless DTC-SVM for induction motor driven by a matrix converter using a parameter estimation strategy. IEEE T Ind Electron 2008; 55: 512-521.

[21] Hamouda M, Blanchette HF, Al-Haddad K. Indirect matrix converters enhanced commutation method. IEEE T Ind Electron 2015; 62: 671-679.